Generation of trans-mitochondrial mito-mice by the introduction of a pathogenic G13997A mtDNA from highly metastatic lung carcinoma cells

Mutsumi Yokota[a,b,†], Hiroshi Shitara[c,†], Osamu Hashizume[a], Kaori Ishikawa[a], Kazuto Nakada[a], Rie Ishii[c], Choji Taya[c], Keizo Takenaga[d], Hiromichi Yonekawa[c], and Jun-Ichi Hayashi[a,*]

[a] *Graduate School of Life and Environmental Sciences, University of Tsukuba, 1-1-1 Tennodai, Tsukuba, Ibaraki 305-8572, Japan.*

[b] *Japan Society for the Promotion of Science (JSPS), 8 Ichiban-cho, Chiyoda-ku, Tokyo 102-8472, Japan.*

[c] *Laboratory for Transgenic Technology, The Tokyo Metropolitan Institute of Medical Science, Tokyo 113-8613, Japan*

[d] *Shimane University Faculty of Medicine, 89-1 Enya-cho, Izumo, Shimane 693-8501, Japan.*

[†] *Both authors contributed equally to this study.*

* Corresponding author. Tel: +81 298536650; Fax: +81 298536650; E-mail: jih45@biol.tsukuba.ac.jp

ABSTRACT

To investigate the effects of respiration defects on the disease phenotypes, we generated trans-mitochondrial mice (mito-mice) by introducing a mutated G13997A mtDNA, which specifically induces respiratory complex I defects and metastatic potentials in mouse tumor cells. First, we obtained ES cells and chimeric mice containing the G13997A mtDNA, and then we generated mito-mice carrying the G13997A mtDNA *via* its female germ line transmission. The three-month-old mito-mice showed complex I defects and lactate overproduction, but showed no other phenotypes related to mitochondrial diseases or tumor formation, suggesting that aging or additional nuclear abnormalities are required for expression of other phenotypes.

Keywords: somatic mtDNA mutation; metastasis; mtDNA transfer; trans-mitochondrial mito-mice

1. Introduction

Pathogenic mtDNA mutations that induce significant respiration defects are responsible for expression of mitochondrial diseases [1-3]. Moreover, such respiration defects and the resultant over production of reactive oxygen species (ROS) and lactate could also be involved in aging, age-associated disorders, and tumor development [2-5]. However, because of the control of the mitochondrial respiratory function by both nuclear DNA and mtDNA [1, 2], it has been difficult to determine which genome, nuclear DNA or mtDNA, is responsible for the respiration defects and the resultant abnormalities.

Our previous study [6] resolved this issue by using complete mtDNA exchange technology between two mouse lung carcinoma cell lines, P29 and A11, which express different metastatic phenotypes. The results showed that the highly metastatic A11 cells possess a somatic mtDNA mutation G13997A in the *ND6* gene that encodes NADH dehydrogenase subunit 6, one of the subunits of respiration complex I, and that the mutation reversibly controls development of metastases in tumor cells. Moreover, the induction of metastasis in the tumor cells was due to the complex I defects-mediated overproduction of ROS, but not to the complex I defects-mediated overproduction of lactate [7]. In humans, complex I defects caused by pathogenic mtDNA mutations are also thought to be responsible for expression of Leber's hereditary optic neuropathy (LHON), one of the most frequent mitochondrial diseases [1-3].

Therefore, generation of trans-mitochondrial mito-mice possessing the G13997A mtDNA introduced from highly metastatic tumor cells would provide an ideal system to examine whether somatic mtDNA mutations introduced from highly metastatic tumor cells into ES cells can be transmitted to the following generations, and

whether they can induce complex I defects in living mouse tissues and induce phenotypes related to LHON, aging, and metastasis. Here, we generated the trans-mitochondrial mito-mice with homoplasmic G13997A mtDNA in all the tissues using mtDNA transfer technology, and then examined the resultant phenotypes.

2. Materials and Methods

2.1. Cell lines and cell culture

Mouse tumor cells were grown in RPMI 1640 (Nissui Seiyaku, Tokyo, Japan) containing 10% fetal calf serum, uridine (50 ng/ml), and pyruvate (0.1 μg/ml). Mouse ES cells (TT2-F, an XO subline established from XY TT2 cells [8]) and mtDNA-repopulated ES cells were cultivated on mitomycin C-inactivated feeder cells derived from fetal fibroblasts, in Dulbecco's Modified Eagle Medium (DMEM; Invitrogen, Carlsbad, CA, USA) supplemented with 15% KNOCKOUT^{TM} Serum Replacement (Invitrogen), 1× non-essential amino acids (MP Biomedicals LLC, OH, USA), leukemia inhibitory factor (10^5 units/ml, Invitrogen), and 100 μM 2-mercaptoethanol (Sigma-Aldrich, St. Louis, MO, USA).

2.2. Isolation of ESmt13997 cells carrying the imported G13997A mtDNA

The host ES cells were pretreated with rhodamine 6G (R6G; 0.38 to 1.5 μg/ml in 3% ethanol) for 48 h in medium supplemented with uridine (50 ng/ml) and pyruvate (0.1 μg/ml) to eliminate endogenous mitochondria and mtDNA [9, 10]. The ES cells were then washed with phosphate-buffered saline (PBS) and suspended in R6G-free medium for 2 h to allow recover. The mtDNA donor B82mtA11 cells pretreated with

cytochalasin B (10 μg/ml) for 10 min were centrifuged at 15000g for 30 min at 37°C for enucleation. The resultant cytoplasts were fused with R6G-pretreated ES cells using polyethylene glycol, and the fusion mixture was cultivated in selective medium with HAT (hypoxanthine aminopterin thymidine). Seven days after fusion, growing colonies were picked up for further examination.

2.3. Generation of founder chimeric mice and mito-mice13997

After frozen 8-cell-stage embryos of ICR strain mice (ARK Resource Co., Ltd., Kumamoto, Japan) were thawed, their zona pellucidae were removed by treatment with acidified Tyrode's buffer (Sigma-Aldrich). Each treated embryo was placed with 10 ESmt13997 cells in an indentation well of a 35-mm culture dish and cultured overnight to enable aggregation. The next day, the embryos were transferred into pseudopregnant ICR females (Japan SLC). The resultant progeny were identified by their coat-color chimerism. Founder (F_0) chimeric females were mated with C57BL/6J (B6; CLEA Japan) males to produce the F_1 generation, and the F_1 female mice were backcrossed with B6 males. The F_3 generation was used for further analyses.

2.4. Genotyping of mtDNAs

To detect the presence of the G13997A mutation, a 147-bp fragment containing the 13997 site was amplified by PCR. The nucleotide sequences from nucleotide position 13963 to 13996 (5′-CCCACTAACAATTAAACCTAAACCTCCATActTA-3′, small letters indicate the mismatch site) and nucleotide position 14109 to 14076 (5′-TTCATGTCATTGGTCGCAGTTGAATGCTGTGTAG-3′) were used as oligonucleotide primers. Combination of the PCR-generated mutation with the G13997A mutation creates a restriction site for *Afl* II, and generates 114-bp and 33-bp

fragments on *Afl* II digestion. The restriction fragments were separated by electrophoresis in a 3% agarose gel. For quantification of the G13997A mtDNA, we used the NIH IMAGE program.

2.5. Analysis of multipotency of mtDNA-repopulated ES cells

To test the multipotency of the mtDNA-repopulated ES cells, ES cells and ESmt13997 cells, 1×10^6 cells of each, were inoculated subcutaneously into the backs of 6-week-old nude mice (JCL, BALB/c-nu/nu; CLEA Japan). The resulting teratomas (tumors) were fixed in 30% neutral-buffered formalin, embedded in paraffin, stained with hematoxylin and eosin (HE) and examined histologically.

2.6. Biochemical measurement of respiratory enzyme activities

Mitochondrial respiratory complex I (NADH dehydrogenase), complex II (succinate dehydrogenase), complex III (cytochrome *c* reductase), and complex IV (cytochrome *c* oxidase) are components of the electron-transport chain, and are located in the mitochondrial inner membrane. The activity of these enzymes was assayed as described previously [11]. Briefly, for the estimation of complex I + III activity, NADH and cytochrome *c* (oxidized form) were used as substrates and the reduction of cytochrome *c* was monitored by measuring absorbance at 550 nm. For the estimation of complexes II + III activity, sodium succinate and cytochrome *c* (oxidized form) were used as substrates, and the reduction of cytochrome *c* was monitored as described above. For the estimation of complex IV activity, cytochrome *c* (reduced form) was used as a substrate, and the oxidation of cytochrome *c* was measured at 550 nm.

2.7. Lactate measurement

To determine fasting blood lactate concentrations, blood was collected from the tail veins of mice after overnight starvation. After oral administration of glucose (1.5 g/kg body weight), blood was again collected, and lactate concentrations were measured using an automatic blood lactate test meter (Lactate Pro, ARKRAY, Kyoto, Japan).

2.8. Measurement of ROS production

ROS generation was detected with 2′,7′-dichlorofluorescin diacetate (DCFH-DA; Molecular Probe, Inc., Eugene, OR, USA). Cells were incubated with DCFH-DA, washed twice, and then immediately analyzed by using a FACScan flow cytometer (Becton Dickinson, Mountain View, CA, USA).

2.9. Western blot analysis of ROS scavenger enzymes

Tissue samples were lysed on ice in 2% SDS (Wako, Osaka, Japan), 50 mM Tris–HCl (pH 6.8), 10% Glycerol (Wako), 5% 2-Mercaptoethanol (Wako) and 0.02% Bromophenol Blue (Wako). After centrifugation at 45,000 rpm for 30 min at 4 °C, the supernatant was used as a protein sample. For Western blot analysis of manganese superoxide dismutase (MnSOD), glutathione peroxidase (GPx), and catalase, the proteins were resolved by SDS-PAGE under reducing conditions. The resolved proteins were transferred electrophoretically to a nitrocellulose membrane (GE Healthcare Bio-Science KK, Tokyo, Japan). The membrane was incubated with either anti-MnSOD antibody (Upstate Biotechnology, Lake Placid, NY, USA), anti-Glutathione Peroxidase 1 antibody (Abcam, Cambridge, UK), or anti-Catalase antibody (Calbiochem, Darmstadt, Germany) for 2 h. Proteins were detected using Immunostaining HRP-1000 (Konica Minolta, Tokyo, Japan). An anti-β-actin antibody (Sigma-Aldrich) was used for the loading control.

2.10. Histological analysis of eyes

Eyes with attached optic nerves were fixed in 30% neutral-buffered formalin and embedded in paraffin. Cross-sections of the optic nerve and horizontal sections of the retina were stained with HE for light microscopic examination.

3. Results

3.1. Isolation of trans-mitochondrial ES cells carrying G13997A mtDNA

To obtain trans-mitochondrial ES cells carrying the G13997A mtDNA (ESmt13997 cells), we used mouse ES cells and mouse B82mtA11 cells as the recipients and the donors of the G13997A mtDNA, respectively (Supplementary Table 1). The B82mtA11 cells were isolated previously [6] by fusing enuclated A11 cells with mtDNA-less B82 cells. Since the B82mtA11 cells could not survive in the selection medium with HAT, they could be used as mtDNA donors for mouse ES cells (Supplementary Table 1).

ES cells were pretreated with R6G to eliminate endogenous mitochondria and mtDNA, and then fused with enucleated B82mtA11 cells. Unfused R6G-pretreated ES cells failed to grow due to the absence of mitochondria and mtDNA, and unenucleated B82mtA11 cells failed to grow by the HAT selection (Supplementary Table 1).

Growing colonies in the selection medium were clonally isolated, and seven clones were used for mtDNA genotyping. All seven clones possessed various proportions of the imported G13997A mtDNA (Fig. 1A). The mtDNA without the

mutation in these clones would be derived from feeder cells or ES cells carrying their own mtDNA due to incomplete R6G pre-treatment. We selected two clones, ESmt13997-5 and -7, which possessed 55% and 85% G13997A mtDNA, respectively, as ESmt13997 cells for use in further experiments.

3.2. Effects of the imported G13997A mtDNA on differentiation of the ESmt13997 cells

In previous reports [12-14], chimeric mice were not obtained from trans-mitochondrial ES cells carrying the pathogenic mtDNAs that induce significant respiration defects, suggesting that significant respiration defects inhibited the differentiation of multipotent ES cells. Therefore, we tested whether the ESmt13997 cells are able to differentiate into various tissues, by subcutaneously inoculating ESmt13997-7 cells into the back skin of nude mice. They formed primary tumors, which grew faster than those of the ES cells with wild-type mtDNA (Supplementary Fig. 1A). Faster growth of the inoculated ESmt13997 cells would be due to the induction of hypoxia-resistant phenotypes in the cells with the G13997A mtDNA [6].

Histological analysis of the primary tumors showed that both the ESmt13997-7 cells and the ES cells with wild-type mtDNA were capable of differentiation into multiple tissue types, such as secretory cells, bone cells, striated muscle, and hair follicles (Supplementary Fig. 1B), even though ESmt13997-7 cells showed faster growth as primary tumors (Supplementary Fig. 1A). These observations suggested that the ESmt13997 cells could be used to obtain F_0 chimeric mice.

3.3. Generation of mito-mice13997 carrying homoplasmic G13997A mtDNA

To generate F_0 chimeric mice, ESmt13997-5 and -7 cells were aggregated with 8-cell-stage embryos of ICR strain mice. We obtained 24 F_0 chimeric mice (11 females and 13 males) showing 5% to 90% chimerism by coat color (Table 1). The results of mtDNA genotyping showed that 5 of 13 F_0 males and 6 of 11 F_0 females possessed 1% to 43% G13997A mtDNA in their tails (Table 1). Because mouse mtDNA inherits strictly maternally [15, 16], we used all 11 F_0 females as founders, irrespective of whether their tails possessed the G13997A mtDNA or not, and mated them with B6 males for examination of its female germ line transmission to the F_1 progeny.

Of the 11 F_0 females, only one produced F_1 pups (2 females and 5 males) that possessed homoplasmic G13997A mtDNA in their tails (Table 1). This F_0 female was derived from the ES mt13997-5 clone carrying 55% G13997A mtDNA. Probably, the ESmt13997-5 possessed homoplasmic G13997A mtDNA, and estimation of 55% G13997A mtDNA in the clone sample (Fig. 1A) was due to the presence of feeder cells.

Then, we examined one of the F_1 males with homoplasmic G13997A mtDNA in its tail, and showed that all tissues tested possessed homoplasmic G13997A mtDNA (Fig. 1B). This finding suggests that the G13997A mtDNA transmitted maternally from an F_0 female to F_1 progeny, and that the F_1 mice carry the G13997A mtDNA originally derived from highly metastatic Lewis lung carcinoma A11 cells. Mice carrying the homoplasmic G13997A mtDNA in all tissues were named mito-mice13997.

Our previous reports [12, 17] showed that mito-mice generated by introduction of the mtDNA with a large-scale deletion (ΔmtDNA) into fertilized eggs did not possess homoplasmic ΔmtDNA, because the ΔmtDNA induced embryonic lethality. Thus,

generation of the F_1 mice carrying homoplasmic G13997A mtDNA (Fig. 1B) indicates that the pathogenicity of the G13997A mtDNA was not sufficient to induce embryonic lethality.

We mated two F_1 female mito-mice13997 with B6 males and obtained F_2 progeny. Then, we obtained F_3 progeny from seven F_2 females. Three-month-old male mito-mice13997 of the F_3 generation were used for further examination of respiratory function and disease phenotypes, while female mito-mice13997 were used to breed and maintain the mito-mice13997 line. Genotyping of mtDNA in one of the F_3 males confirmed homoplasmic G13997A mtDNA in all the tissues tested (Fig. 1C).

3.4. Mitochondrial dysfunction and disease phenotypes in the mito-mice13997

Using the mito-mice13997 (three-month-old F_3 males), first we analyzed respiratory complex activities in various tissues. Tissues from age-matched B6 mice were used as normal controls. The activity levels of complexes II + III and complex IV in the tissues of mito-mice13997 were not significantly different to normal levels (Fig. 2A). In contrast, all mito-mice13997 tissues tested showed significantly less complex I + III activity (about 70% normal level). Since the activity of complexes II + III was normal in the mito-mice13997 tissues, we consider that the reduced activity of complexes I + III reflects complex I activity alone.

Our previous study [6] showed that complex I defects caused by the G13997A mtDNA induced simultaneous overproduction of ROS and lactate in cultivated tumor cells. So, we estimated the amounts of ROS in the liver cells and splenocytes of the

mito-mice13997 by means of fluorescence-activated cell sorting (FACS; Fig. 2B). The results showed no significant increase in the amount of ROS in the mito-mice13997 tissues compared to the control B6 mice. Moreover, the levels of antioxidant enzymes, such as MnSOD, GPx, and catalase in the liver cells and splenocytes of the mito-mice13997 were not significantly different to those in the control B6 mice (Fig. 2C). Thus, the tissues in living mice may have some systems other than the enhanced expression of anti-oxidant enzymes that suppress the ROS overproduction caused by the mutated mtDNA.

In contrast, after glucose loading, the lactate level in blood was significantly higher in mito-mice13997 than in control B6 mice (Fig. 3A). This phenotype is also found in other mito-mice [13, 17]. Moreover, in human cases, lactic acidosis is one of the most common phenotypes in the patients with mitochondrial diseases [1-3], and our results suggest that the mito-mice13997 can be used as models of lactic acidosis.

In humans, complex I defects caused by mtDNA mutations are also associated with LHON [1-3]. The typical clinical features of LHON are loss of central vision and optic nerve atrophy in young males due to the selective loss of retinal ganglion cells, which histologically correspond to the loss of the optic nerve and the loss of both the nerve fiber layer and ganglion cell layer in the retina [18]. So, we histologically examined the retinal ganglion cells in three-month-old male mito-mice13997. The results showed normal optic nerve in the size and nerve fiber density (Fig. 3B upper panels), and normal histology in both the nerve fiber layer and ganglion cell layer in the retina (Fig. 3B lower panels). These histological observations indicated that the male

mito-mice13997 did not express the typical phenotypes of LHON [18] at least 3 months after birth.

Finally we examined the tendency to form tumors using three-month-old mito-mice13997 of F_3 generation, since their G13997A mtDNA was derived from highly metastatic Lewis lung carcinoma A11 cells, and they showed high lactate levels in the blood (Fig. 3A). However, all six mito-mice13997 tested showed no bias towards the preferential formation of tumors. These results can be explained by the fact that the G13997A mtDNA induces metastasis in tumor cells, but does not induce tumor development in normal cells [6].

4. Discussion

Because mouse G13997A mtDNA in highly metastatic tumor cells induces respiratory complex I defects and leads to overproduction of ROS and lactates [6, 7], we expected that the generation of the mito-mice13997 with homoplasmic G13997A mtDNA would be an effective means to examine the conventional mitochondrial theories [2-5] proposing that ROS and lactate overproduction caused by pathogenic mtDNA mutations is responsible for aging, age-associated disorders, and tumor development.

As expected, the mito-mice13997 showed complex I defects (Fig. 2A) and resultant overproduction of lactate (Fig. 3A). However, the deficiency in complex I activity was less in mito-mice13997 tissues than in the mtDNA donor B82mtA11 cells (Fig. 2A). A similar compensatory effect was observed, when mito-mice6589 tissues

expressing complex IV defects due to homoplasmic T6589C mtDNA mutation in the *COI* gene were compared to their mtDNA donor cells [13]. Thus, the tissues in living mice may have some activities that compensate for the reduced respiration defects caused by pathogenic mtDNA mutations.

In addition, ROS overproduction, LHON phenotypes, and tumor formation were not observed in the mito-mice13997. Probably, the tissues in living mice are capable not only of compensating for reduced complex I activity, but also of suppressing ROS overproduction. In this study we used young mito-mice13997 to examine these phenotypes. Thus, we cannot at present exclude the possibility that aging of mito-mice13997 abolishes the compensatory function in the young tissues, resulting in expression of these phenotypes in aged mito-mice13997.

With respect to the LHON phenotypes, it has been proposed that a mutation in either the *ND1*, *ND4*, or *ND6* gene of mtDNA is necessary, but not sufficient to express LHON phenotypes, and that some additional nuclear gene mutations are required [1-3]. Hence, addition of similar nuclear gene mutations may induce the LHON phenotypes in the mito-mice13997. The absence of tumor formation in the mito-mice13997 suggests that increased lactate levels in the presence of oxygen, which is known as the Warburg effect [19], were not sufficient to induce tumor formation in the mito-mice13997. Since our previous report [6] showed that the G13997A mtDNA induces metastasis in tumor cells, but does not induce tumor formation in normal cells, it can be expected that the mito-mice13997 would not show tumor formation, but would show high metastasis, only when nuclear gene mutations or a different nuclear background that preferentially induce tumor formation were introduced.

Therefore, aging of the mito-mice13997 and/or the introduction of different nuclear backgrounds or nuclear gene abnormalities into the mito-mice13997 would be important for further investigation of the capability of the mito-mice13997 to express significant complex I defects, ROS overproduction, tumor formation, metastasis, and the phenotypes related to LHON and aging.

5. Acknowledgements

This work was supported by Grants-in-Aid for Scientific Research (S) from the Japan Society for Promotion of Science (JSPS) to J.-I.H. This work was also supported by grants for a Research Fellowship from JSPS for Young Scientists to M.Y. and to K. I. This work was partly supported by a Grant-in-Aid for Cancer Research (21-1-①) from the Ministry of Health, Labor and Welfare of Japan, and by the Research Grant (20B-13) for Nervous and Mental Disorders from the Ministry of Health, Labor and Welfare to K.N.

6. References

[1] Larsson, N.-G. and Clayton, D.A. (1995). Molecular genetic aspects of human mitochondrial disorders. *Annu. Rev. Genetics* 29, 51-178.

[2] Wallace, D.C. (1999). Mitochondrial diseases in man and mouse. *Science* 283, 1482-1488.

[3] Taylor, R.W. and Turnbull, D.M. (2005). Mitochondrial DNA mutations in human disease. *Nature Rev. Genet.* 6, 389-402.

[4] Jacobs, H.T. (2003). The mitochondrial theory of aging: dead or alive? *Aging Cell* 2, 11-17.

[5] Loeb, L.A., Wallace, D.C., and Martin, G.M. (2005). The mitochondrial theory of aging and its relationship to reactive oxygen species damage and somatic mtDNA mutations. *Proc. Natl. Acad. Sci. USA* 102, 18769-18770.

[6] Ishikawa, K., Takenaga, K., Akimoto, M., Koshikawa, N., Yamaguchi, A., Imanishi, H., Nakada, K., Honma, Y., and Hayashi, J.-I. (2008). ROS-generating mitochondrial DNA mutations can regulate tumor cell metastasis. *Science* 320, 661-664.

[7] Ishikawa, K., Hashizume, O., Koshikawa, N., Fukuda, S., Nakada, K., Takenaga, K., and Hayashi, J.-I. (2008). Enhanced glycolysis induced by mtDNA mutations does not regulate metastasis. *FEBS Lett.* 582, 3525-3530.

[8] Yagi, T., Tokunaga, T., Furuta, Y., Nada, S., Yoshida, M., Tsukada, T., Saga, Y., Takeda, N., Ikawa, Y. and Aizawa, S. (1993). A novel ES cell line, TT2, with high germline-differentiating potency. *Anal. Biochem*. 214, 70–76.

[9] Ziegler, M.L. and Davidson, R.L. (1981). Elimination of mitochondrial elements and improved viability in hybrid cells. *Somatic Cell Genet*. 7, 73-88.

[10] McKenzie, M., Trounce, I.A., Cassar, C.A. and Pinkeert, C.A. (2004). Production of homoplasmic xenomitochondrial mice. *Proc. Natl. Acad. Sci. USA* 101: 1685-1690.

[11] Miyabayashi S., Haginoya K., Hanamizu H., Iinuma K., Narisawa K., and Tada K. (1989). Defective pattern of mitochondrial respiratory enzymes in mitochondrial myopathy. *J. Inherit. Metab. Dis*. 12, 373-377.

[12] Ishikawa, K., Kasahara, A., Watanabe, N., Nakada, K., Sato, A., Suda, Y., Aizawa, S., and Hayashi, J.-I. (2005). Application of ES cells for generation of respiration-deficient mice carrying mtDNA with a large-scale deletion. *Biochem. Biophys. Res. Commun.* 333, 590-595.

[13] Kasahara, A., Ishikawa, K., Yamaoka, M., Ito, M., Watanabe, N., Akimoto, M., Sato, A., Nakada, K., Endo, H., Suda, Y., Aizawa, S. and Hayashi, J.-I. (2006). Generation of trans-mitochondrial mice carrying homoplasmic mtDNAs with a missense mutation in a structural gene using ES cells. *Hum. Mol. Genet.* 15, 871-881.

[14] Fan, W., Waymire, K.G., Narula, N., Li, P., Rocher, C., Coskun, P.E. Vannan, M.A., Narula J., MacGregor, G.R. and Wallace, D.C. (2008). A mouse model of mitochondrial disease reveals germline selection against severe mtDNA mutations. *Science* 319, 958-962.

[15] Kaneda, H., Hayashi, J.-I., Takahama, S., Taya, C., Fischer Lindahl, K., and Yonekawa, H. (1995). Elimination of paternal mitochondrial DNA in

intraspecific crosses during early mouse embryogenesis. *Proc. Natl. Acad. Sci. USA* 92, 4542-4546.

[16] Shitara, H., Hayashi, J.-I., Takahama, S., Kaneda, H., and Yonekawa, H. (1998). Maternal inheritance of mouse mtDNA in interspecific hybrids: segregation of the leaked paternal mtDNA followed by the prevention of subsequent paternal leakage. *Genetics* 148, 851-857.

[17] Inoue K, Nakada K, Ogura A, Isobe K, Goto Y, Nonaka I, and Hayashi J.-I. (2000). Generation of mice with mitochondrial dysfunction by introducing mouse mtDNA carrying a deletion into zygotes. *Nature Genet.* 26, 176-181.

[18] Carelli, V., Ross-Cisneros, F.N., and Sadun, A.A. (2004). Mitochondrial dysfunction as a cause of optic neuropathies, *Prog. Retin. Eye Res*. 23, 53–89.

[19] Gottlieb, E., and Tomlinson, I.P. (2005). Mitochondrial tumor suppressors: a genetic and biochemical update. *Nat. Rev. Cancer* 5, 857-866.

7. Figure legends

Fig. 1. The mtDNA genotyping of ESmt13997 and mito-mice13997.

Genotyping of mtDNA from (A) ESmt13997 clones, (B) F_1 male tissues, and (C) F_3 male tissues. PCR products were digested with *Afl* II. The G13997A mtDNA produced 114- and 33-bp fragments due to the gain of an *Afl* II site by the G13997A substitution in the *ND6* gene, whereas wild-type mtDNA without the mutation produced a 147-bp fragment. B82mtA11 cells with homoplasmic G13997A mtDNA were used as positive controls, and ES cells and B82mtB6 cells with wild-type mtDNA were used as negative controls. Br, brain; He, heart; Li, liver; Ki, kidney; Sk, skeletal muscle; Te, testis.

Fig. 2. Phenotypes related to mitochondrial respiratory function.

Open bars, samples with wild-type mtDNA; solid bars, samples with the G13997A mtDNA. Mit represents mito-mice13997. B82mtA11 cells with the G13997A mtDNA and B82mtB6 cells with wild-type mtDNA shared the same nuclear background, and were used to compare relative complex I activity and the amounts of ROS between cultivated cells with and without the G13997A mutation. (A) Biochemical analysis of respiratory complex activities. Respiratory complex I+III, II+III, and IV activities were examined using tissues of the mito-mice13997. Data are presented as mean values with SD (n=3), *P < 0.05 compared with control group. (B) Flow-cytometric analysis of ROS production. We treated B82mtA11 cells, B82mtB6 cells, liver cells and splenocytes with DCFH-DA, and carried out flow-cytmetric analysis for quantitative estimation of H_2O_2. Liver cells were obtained from homogenized tissue in a buffer containing collagenase. Data are presented as mean values with SD (n=3), **P < 0.005 compared with control group. (C) Quantitative estimation of the amounts of ROS scavenger enzymes, MnSOD, GPx, and catalase by Western blot analysis using β-actin as a loading control. No signals of MnSOD and catalase were detectable in the splenocytes. Data are presented as mean values with SD (n=3).

Fig. 3. Phenotypes related to mitochondrial diseases.

(A) Estimation of the amount of lactate in the blood of 3-month-old B6 male mice (open circles) and age-matched male mito-mice13997 (closed circles) before and after glucose loading. Data are presented as mean values with SD (n=3), *P < 0.05 compared with control group. (B) Histological analysis of the optic nerve (upper panels, cross-section)

and the retina (lower panels, horizontal section) after HE staining. NFL, nerve fiber layer; GCL, ganglion cell layer; IPL, internal plexiform layer; INL, internal nuclear layer; OPL, outer plexiform layer; ONL, outer nuclear layer. Bar, 100 μm (upper panels); Bar, 10 μm (lower panels).

Supplementary Fig. 1. Effects of the G13997A mtDNA introduced from tumor cells into ESmt13997 cells on their differentiation.

Left panels, ES cells; right panels, ESmt13997-7 cells possessing the introduced G13997A mtDNA. (A) The primary tumor masses formed in nude mice. Bar, 1 cm. (B) Histological analysis of the primary tumor masses after HE staining. Panels *a, b, c*, and *d* correspond to secretory cells, bone cells, striated muscles, and hair follicles, respectively. Bar, 100 μm.

Table 1
Generation of F_0 chimeric mice and their F_1 progeny carrying the G13997A mtDNA in tails

ES cells		F_0 mice		F_1 mice
ES clone	% G13997A mtDNA	% Chimerism	% G13997A mtDNA in the tails	No. of F_1 mice with G13997A mtDNA in the tails / No. of F_1 mice
ESmt13997-5	55	40 (♀)	0	0 / 35
		40 (♀)	0	0 / 41
		50 (♀)	21	0 / 46
		50 (♀)	0	0 / 40
		50 (♀)	11	0 / 58
		50 (♀)	15	0 / 38
		80 (♀)	0	0 / 63
		80 (♀)	26	7[a] / 23
		20 (♂)	0	
		20 (♂)	0	
		20 (♂)	0	
		20 (♂)	0	
		20 (♂)	0	
		30 (♂)	0	
		30 (♂)	19	
		80 (♂)	23	
ESmt13997-7	85	5 (♀)	0	0 / 61
		40 (♀)	13	0 / 55
		90 (♀)	43	0 / 12
		5 (♂)	0	
		5 (♂)	1	
		10 (♂)	0	
		20 (♂)	6	
		30 (♂)	4	

[a] Seven out of 23 F_1 mice possessed homoplasmic G13997A mtDNA in their tails. Two were females and five were males. We used these two F_1 females for breeding, and obtained F_2 mito-mice13997. All F_2 mito-mice13997 possessed homoplasmic G13997A mtDNA in their tails. The number of F_3 pups and their body weight were comparable to those of B6 mice.

Fig. 1.

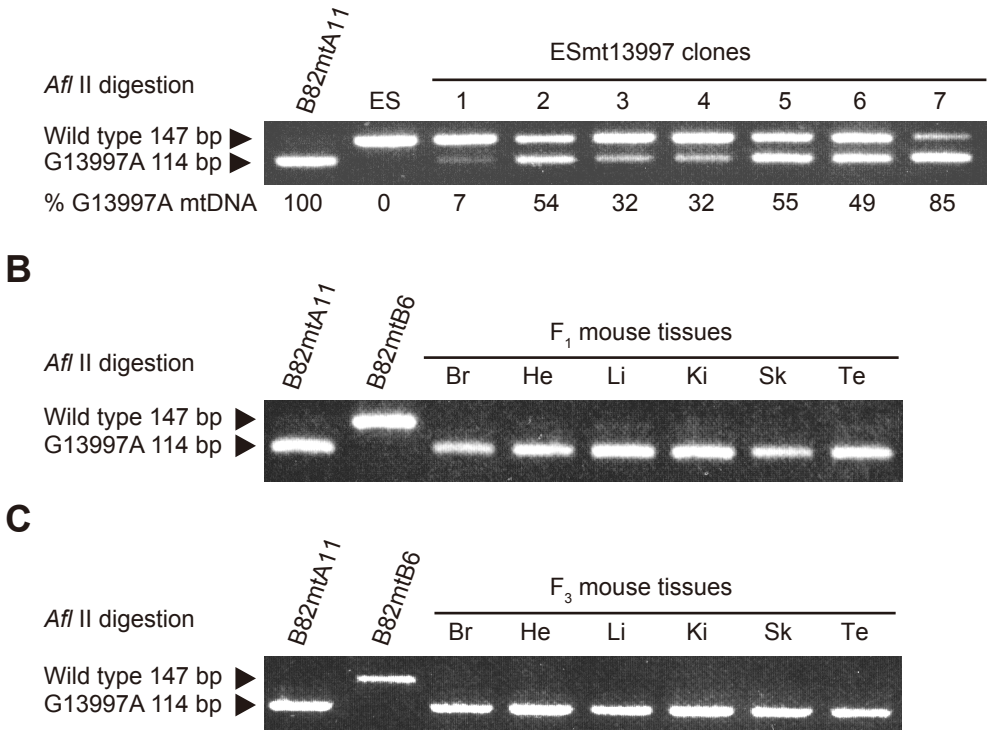
A
AflII digestion
B82mtA11
ES
ESmt13997 clones
1
2
3
4
5
6
7
Wild type 147 bp
G13997A 114 bp
% G13997A mtDNA
100
0
7
54
32
32
55
49
85
B
AflII digestion
B82mtA11
B82mtB6
F1 mouse tissues
Br
He
Li
Ki
Sk
Te
Wild type 147 bp
G13997A 114 bp
C
AflII digestion
B82mtA11
B82mtB6
F3 mouse tissues
Br
He
Li
Ki
Sk
Te
Wild type 147 bp
G13997A 114 bp

Fig. 2.

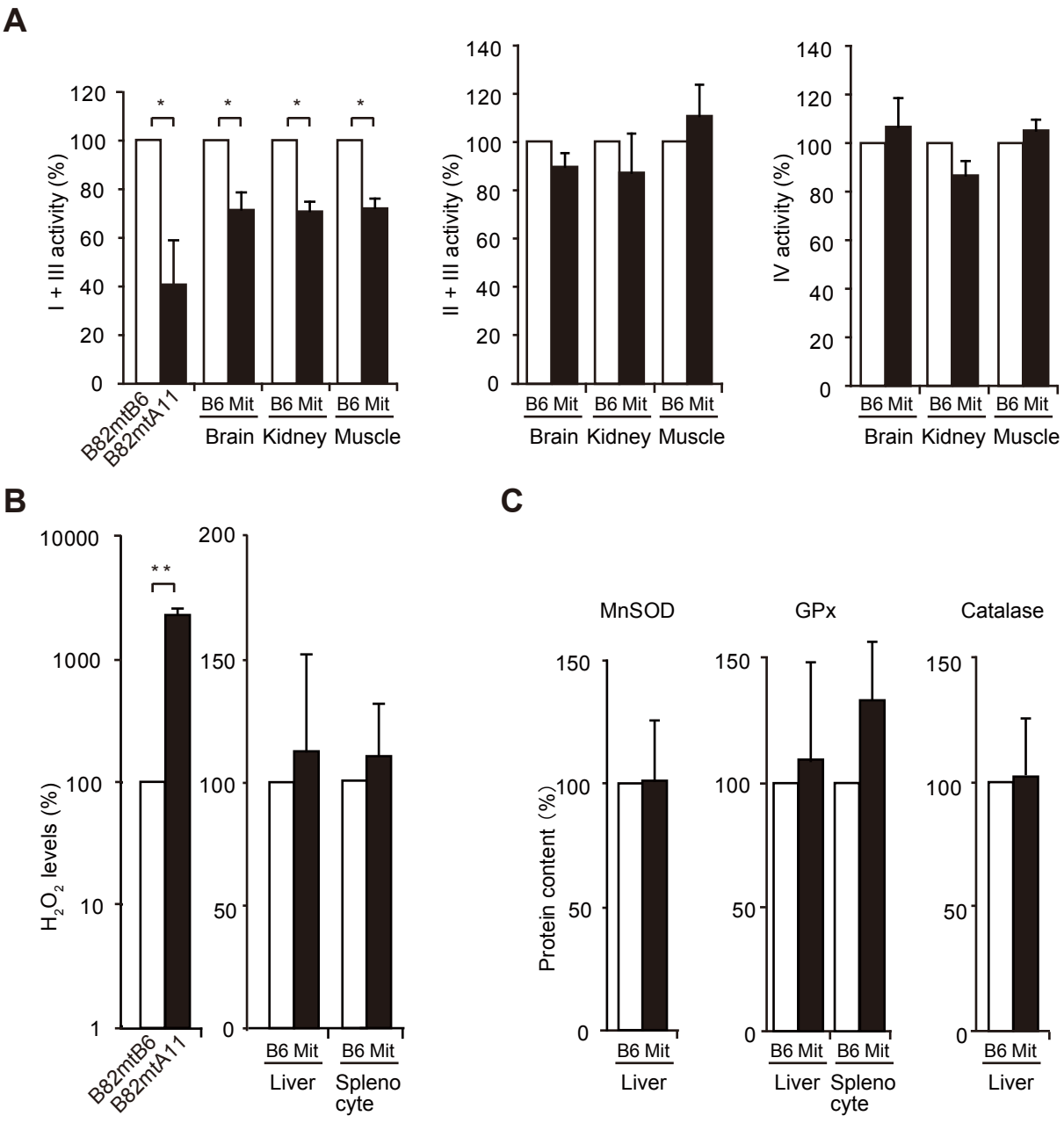
A
I + III activity (%)
II + III activity (%)
IV activity (%)
B82mtB6
B82mtA11
B6 Mit
Brain
Kidney
Muscle
B
H_2O_2 levels (%)
Liver
Spleno cyte
C
MnSOD
GPx
Catalase
Protein content (%)

Fig. 3.

A

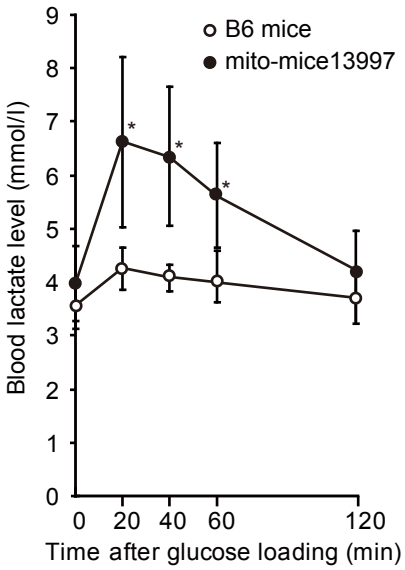
B6 mice
mito-mice13997
Blood lactate level (mmol/l)
0
1
2
3
4
5
6
7
8
9
0
20
40
60
120
Time after glucose loading (min)
*
*
*

B

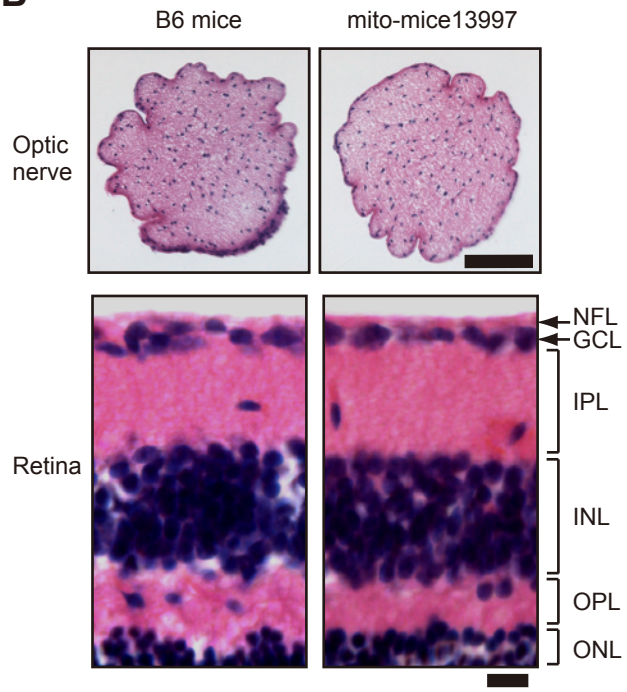
B6 mice
mito-mice13997
Optic nerve
Retina
NFL
GCL
IPL
INL
OPL
ONL

Supplementary Table 1

Genetic characteristics of the nuclear donors, mtDNA donors , and resultant trans-mitochondrial ES cells (ESmt13997)

Cell lines	Nuclear genotypes	mtDNA genotypes	Fusion combination			Selection
			Nuclear donors	×	mtDNA donors	
Nuclear donors						
R6G-ES[a]	HAT resistant	without mtDNA				
mtDNA donors						
B82mtA11[b]	HAT sensitive	G13997A				
Trans-mitochondrial ES cells						
ESmt13997	HAT resistant	G13997A	en B82mtA11[c]	×	R6G-ES	HAT[d]

[a] ES cells pretreated with R6G to exclude endogenous mitochondria and mtDNA.

[b] The nuclear DNA is derived from B82 cells that are resistant to BrdU and sensitive to HAT, and mtDNA is derived from highly metastatic Lewis lung carcinoma A11 cells possessing the G13997A mtDNA.

[c] en represents enucleation to obtain cytoplasts without nuclei.

[d] To obtain ES cells carrying the G13997A mtDNA (ESmt13997 cells), ES cells were pretreated with R6G to eliminate their mitochondria and mtDNA, and the resultant R6G-ES cells were fused with enucleated B82mtA11 cells. The fusion mixtures were cultivated in HAT selection medium to exclude unenucleated B82mtA11 cells. Unfused R6G-ES cells cannot survive due to the absence of mtDNA and mitochondria.

Supplementary Fig. 1.